van der Waals coupling in atomically doped carbon nanotubes

I.V. Bondarev*
Institute for Nuclear Problems, Belarusian State University, Bobruiskaya Str.11, 220050 Minsk, BELARUS

Ph. Lambin
Facultés Universitaires Notre-Dame de la Paix, 61 rue de Bruxelles, 5000 Namur, BELGIUM

We have investigated atom-nanotube van der Waals (vdW) coupling in atomically doped carbon nanotubes (CNs). Our approach is based on the perturbation theory for degenerated atomic levels, thus accounting for both weak and strong atom-vacuum-field coupling. The vdW energy is described by an integral equation represented in terms of the local photonic density of states (DOS). By solving it numerically, we demonstrate the inapplicability of standard weak-coupling-based vdW interaction models in a close vicinity of the CN surface where the local photonic DOS effectively increases, giving rise to an atom-field coupling enhancement. An inside encapsulation of atoms into the CN has been shown to be energetically more favorable than their outside adsorption by the CN surface. If the atom is fixed outside the CN, the modulus of the vdW energy increases with the CN radius provided that the weak atom-field coupling regime is realized (i.e., far enough from the CN). For inside atomic position, the modulus of the vdW energy decreases with the CN radius, representing a general effect of the effective interaction area reduction with lowering the CN curvature.

PACS numbers: 61.46.+w, 73.22.-f, 68.65.-k, 34.50.Dy

I. INTRODUCTION

Carbon nanotubes (CNs) are graphene sheets rolled-up into cylinders of approximately one nanometer in diameter. Extensive work carried out worldwide in recent years has revealed the intriguing physical properties of these novel molecular scale wires [1, 2]. Nanotubes have been shown to be useful for miniaturized electronic, mechanical, electromechanical, chemical and scanning probe devices and materials for macroscopic composites [3]. Important is that their intrinsic properties may be substantially modified in a controllable way by doping with extrinsic impurity atoms, molecules and compounds [4]. Recent successful experiments on encapsulation of single atoms into single-wall CNs [5] and their intercalation into single-wall CN bundles [4, 6], along with numerous studies of monoatomic gas absorbtion by the CN bundles (see [7] for a review), stimulate an in-depth analysis of the atom-CN van der Waals (vdW) interactions. The problem is both of fundamental and of applied interest, because it sheds light on the peculiarities of the atom-electromagnetic-field interactions in low-dimensional dispersive and absorbing surroundings, on the one hand, and, on the other, the atom-nanotube vdW interaction is the most important one determining the filling factor in encapsulating single atoms into CNs.

The vdW interaction is the result of electrodynamic coupling between the polarization states of the interacting entities that results from the vacuum fluctuations of the electromagnetic field. A theoretical analysis recently done [8, 9, 10] of spontaneous decay dynamics of excited atomic states near CNs has brought out fascinating peculiarities of the vacuum-field interactions in atomically doped CNs. In particular, close to the nanotube, the relative density of photonic states (DOS) effectively increases due to the presence of additional surface photonic states coupled with CN electronic quasiparticle excitations. This causes an atom-vacuum-field coupling constant, which is proportional to the photonic DOS, to be very sensitive to an atom-CN-surface distance. If the atom is close enough to the CN surface and the atomic transition frequency is in the vicinity of a resonance of the photonic DOS, the system shows strong atom-vacuum-field coupling giving rise to rearrangement ("dressing") of atomic levels by the vacuum-field interaction. If the atom moves away from the CN surface, the atom-field coupling strength decreases, smoothly approaching the weak coupling regime at large atom-surface distances since the role of surface photonic states diminishes, causing the relative photonic DOS to decrease. This suggests strictly nonlinear atom-field coupling and a primary role of the distance-dependent (local) photonic DOS in the vicinity of the CN, so that (weak-coupling) vdW interaction models based upon standard vacuum quantum electrodynamics (QED) as well as those using the linear response theory (see [11, 12] for a review) are, in general, inapplicable for an atom in a close vicinity of a carbon nanotube.

To give this issue a proper quantum electrodynamic consideration and thereby to advance in physical understanding the vdW interactions deeper than simple analyzing empirical model potentials [13], we develop a universal quantum approach to the vdW energy calculation of a (two-level) atomic system in the vicinity of an infinitely long single-wall CN. The approach is based upon the perturbation theory for degenerate atomic levels (see, e.g., [14]), thereby allowing one to account for both strong and weak atom-vacuum-field coupling regimes. We derive an integral equation for the vdW energy of the two-level

*Corresponding author. E-mail address: bondarev@tut.by

atomic system near the CN. The equation is represented in terms of the local photonic DOS and is valid for both strong and weak atom-field coupling. By solving it numerically, we demonstrate the inapplicability of weak-coupling-based vdW interaction models in a close vicinity of the nanotube surface. We also show that an inside encapsulation of doped atoms into the nanotube is energetically more favorable than their outside adsorption by the nanotube surface.

The rest of the paper is arranged as follows. Section II presents a theoretical model we use to derive a universal integral equation for the ground-state vdW energy of the two-level atomic system interacting with a vacuum electromagnetic field in the vicinity (inside or outside) of the CN. In describing the atom–field interaction, we follow an original line of Ref. [15, 16], adopting their electromagnetic field quantization scheme for a particular case of the field near an infinitely long achiral single-wall CN. The carbon nanotube is considered to be an infinitely thin anisotropically conducting cylinder. Its surface conductivity is represented in terms of the π-electron dispersion law obtained in the tight-binding approximation with allowance made for azimuthal electron momentum quantization and axial electron momentum relaxation [17]. Only the axial conductivity is taken into account and the azimuthal one, being strongly suppressed by transverse depolarization fields [18, 19, 20, 21], is neglected. In Sec. III, the vdW energy equation derived in Sec. II is analyzed qualitatively to demonstrate its validity and correctness in both weak and strong atom-field coupling regimes. We show that the equation obtained reproduces a well-known perturbation theory result in the weak coupling regime and reduces to the integral equation of a simplified form in the strong coupling regime. Section IV presents and discusses the results of the various numerical calculations of the vdW energies of the two-level atom placed inside or outside achiral CNs of different radii. A summary and conclusions of the work are given in Sec. V.

II. THE GROUND-STATE VAN DER WAALS ENERGY

A. The field quantization formalism

The quantum theory of the van der Waals interaction between an atomic system and a carbon nanotube involves an electromagnetic field quantization procedure in the presence of dispersing and absorbing bodies. Such a procedure faces difficulties similar to those in quantum optics of 3D Kramers-Kronig dielectric media where the canonical quantization scheme commonly used does not work since, because of absorption, corresponding operator Maxwell equations become non-Hermitian [22]. As a consequence, their solutions cannot be expanded in power orthogonal modes and the concept of modes itself becomes more subtle. We, therefore, use a unified

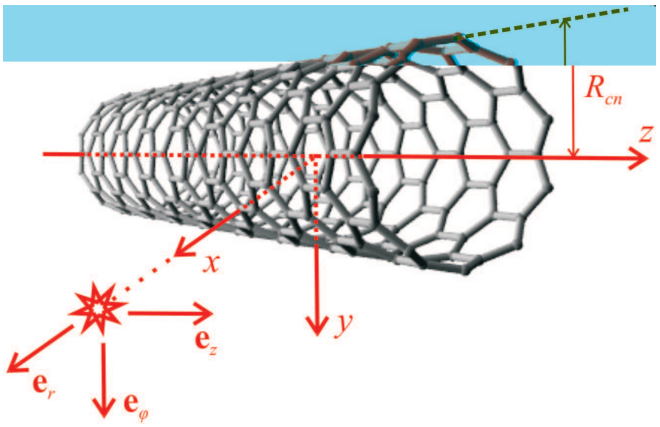

FIG. 1: (Color online) The geometry of the problem.

macroscopic QED approach developed in Refs. [15, 16] and adapted for an atom near a CN in Refs. [9, 10]. In this approach, the Fourier-images of electric and magnetic fields are considered as quantum mechanical observables of corresponding electric and magnetic field operators. The latter ones satisfy the Fourier-domain operator Maxwell equations modified by the presence of a so-called operator noise current density $\hat{\underline{\mathbf{J}}}(\mathbf{r},\omega)$ written in terms of a three-dimensional (3D) vector bosonic field operator $\hat{\mathbf{f}}(\mathbf{r},\omega)$ and a medium dielectric tensor $\boldsymbol{\epsilon}(\mathbf{r},\omega)$ (supposed to be diagonal) as

$$\hat{\underline{J}}_i(\mathbf{r},\omega) = \frac{\omega}{2\pi}\sqrt{\hbar\,\mathrm{Im}\epsilon_{ii}(\mathbf{r},\omega)}\,\hat{f}_i(\mathbf{r},\omega),\ i=1,2,3. \quad (1)$$

This operator is responsible for correct commutation relations of the electric and magnetic field operators in the presence of medium-induced absorbtion. In this formalism, the electric and magnetic field operators are expressed in terms of a continuum set of the 3D vector bosonic fields $\hat{\mathbf{f}}(\mathbf{r},\omega)$ by means of the convolution over $\mathbf{r}$ of the current (1) with the classical electromagnetic field Green tensor of the system. The bosonic field operators $\hat{\mathbf{f}}^\dagger(\mathbf{r},\omega)$ and $\hat{\mathbf{f}}(\mathbf{r},\omega)$ create and annihilate single-quantum electromagnetic medium excitations. They are defined by their commutation relations

$$\begin{aligned}[\,\hat{f}_i(\mathbf{r},\omega),\hat{f}_j^\dagger(\mathbf{r}',\omega')\,] &= \delta_{ij}\delta(\mathbf{r}-\mathbf{r}')\delta(\omega-\omega')\,, \quad (2)\\ [\,\hat{f}_i(\mathbf{r},\omega),\hat{f}_j(\mathbf{r}',\omega')\,] &= [\,\hat{f}_i^\dagger(\mathbf{r},\omega),\hat{f}_j^\dagger(\mathbf{r}',\omega')\,] = 0\end{aligned}$$

and play the role of the fundamental dynamical variables in terms of which the Hamiltonian of the composed system "electromagnetic field + dissipative medium" is written in a standard secondly quantized form as

$$\hat{H} = \int_0^\infty d\omega\,\hbar\omega\int d\mathbf{r}\,\hat{\mathbf{f}}^\dagger(\mathbf{r},\omega)\cdot\hat{\mathbf{f}}(\mathbf{r},\omega)\,. \quad (3)$$

Consider a neutral atomic system with its centre-of-mass positioned at the point $\mathbf{r}_A$ near an infinitely long single-wall CN. Since the problem has a cylindric symmetry, it is convenient to assign the orthonormal cylindric basis $\{\mathbf{e}_r,\mathbf{e}_\varphi,\mathbf{e}_z\}$ in such a way that $\mathbf{e}_z$ is directed

along the nanotube axis and $\mathbf{r}_A = r_A\mathbf{e}_r = \{r_A, 0, 0\}$ (see Fig. 1). For carbon nanotubes, their strong transverse depolarization along with transverse electron momentum quantization allow one to neglect the azimuthal current and radial polarizability [17, 18, 19, 20, 21], in which case the dielectric tensor components ϵ_{rr} and $\epsilon_{\varphi\varphi}$ are identically equal to unit. The component ϵ_{zz} is caused by the CN longitudinal polarizability and is responsible for the axial surface current parallel to the $\mathbf{e}_z$ vector. This current may be represented in terms of the 1D bosonic field operators by analogy with Eq. (1). Indeed, taking into account the dimensionality conservation in passing from bulk to a monolayer in Eq. (3) and using a simple Drude relation [18]

$$\sigma_{zz}(\mathbf{R},\omega) = -i\omega\frac{\epsilon_{zz}(\mathbf{R},\omega)-1}{4\pi S\rho_T}\,, \tag{4}$$

where $\mathbf{R} = \{R_{cn}, \phi, Z\}$ is the radius-vector of an arbitrary point of the CN surface, R_{cn} is the radius of the CN, $\sigma_{zz}(\mathbf{R},\omega)$ is the CN surface axial conductivity per unit length, S is the area of a single nanotube, ρ_T is the tubule density in a bundle, one immediately has from Eq. (1)

$$\hat{\underline{\mathbf{J}}}(\mathbf{R},\omega) = \sqrt{\frac{\hbar\omega \mathrm{Re}\sigma_{zz}(\mathbf{R},\omega)}{\pi}}\,\hat{f}(\mathbf{R},\omega)\mathbf{e}_z \tag{5}$$

with $\hat{f}(\mathbf{R},\omega)$ being the 1D bosonic field operator defined on the CN surface. The total nonrelativistic Hamiltonian of an atomic system interacting with a CN modified quantized vacuum electromagnetic field can then be represented in the form

$$\begin{aligned}\hat{H} &= \int_0^\infty d\omega\,\hbar\omega\int d\mathbf{R}\,\hat{f}^\dagger(\mathbf{R},\omega)\hat{f}(\mathbf{R},\omega)\\ &+ \sum_i \frac{1}{2m_i}\left[\hat{\mathbf{p}}_i - \frac{q_i}{c}\hat{\mathbf{A}}(\hat{\mathbf{r}}_i)\right]^2\\ &+ \frac{1}{2}\int d\mathbf{r}\,\hat{\rho}_A(\mathbf{r})\hat{\varphi}_A(\mathbf{r}) + \int d\mathbf{r}\,\hat{\rho}_A(\mathbf{r})\hat{\varphi}(\mathbf{r})\,,\end{aligned} \tag{6}$$

where m_i, q_i, $\hat{\mathbf{r}}_i$ and $\hat{\mathbf{p}}_i$ are, respectively, the masses, charges, coordinates (relative to $\mathbf{r}_A$) and momenta of the particles constituting the atomic subsystem. The first term of the Hamiltonian describes the *medium-assisted* vacuum electromagnetic field in the presence of the CN. The second and the third terms of the Hamiltonian represent the kinetic energy of the charged particles and their mutual Coulomb interaction, respectively, with

$$\hat{\varphi}_A(\mathbf{r}) = \int d\mathbf{r}'\,\frac{\hat{\rho}_A(\mathbf{r}')}{|\mathbf{r}-\mathbf{r}'|} \tag{7}$$

being the scalar potential and

$$\hat{\rho}_A(\mathbf{r}) = \sum_i q_i\delta(\mathbf{r}-\hat{\mathbf{r}}_i) \tag{8}$$

being the charged density of the atomic subsystem. The last term accounts for the Coulomb interaction of the particles with the CN. The vector potential $\hat{\mathbf{A}}$ and the scalar potential $\hat{\varphi}$ of the CN-modified electromagnetic field are given for an arbitrary $\mathbf{r} = \{r, \varphi, z\}$ in the Schrödinger picture by

$$\hat{\mathbf{A}}(\mathbf{r}) = \int_0^\infty d\omega\frac{c}{i\omega}\,\hat{\underline{\mathbf{E}}}^\perp(\mathbf{r},\omega) + \mathrm{h.c.}, \tag{9}$$

$$-\boldsymbol{\nabla}\hat{\varphi}(\mathbf{r}) = \int_0^\infty d\omega\,\hat{\underline{\mathbf{E}}}^\parallel(\mathbf{r},\omega) + \mathrm{h.c.}, \tag{10}$$

where

$$\hat{\underline{\mathbf{E}}}^{\perp(\parallel)}(\mathbf{r},\omega) = \int d\mathbf{r}'\,\boldsymbol{\delta}^{\perp(\parallel)}(\mathbf{r}-\mathbf{r}')\cdot\hat{\underline{\mathbf{E}}}(\mathbf{r}',\omega) \tag{11}$$

is the transverse (longitudinal) electric field operator with

$$\delta^\parallel_{\alpha\beta}(\mathbf{r}) = -\nabla_\alpha\nabla_\beta\frac{1}{4\pi r} \tag{12}$$

and

$$\delta^\perp_{\alpha\beta}(\mathbf{r}) = \delta_{\alpha\beta}\,\delta(\mathbf{r}) - \delta^\parallel_{\alpha\beta}(\mathbf{r}) \tag{13}$$

being the longitudinal and transverse dyadic δ-functions, respectively, and $\hat{\underline{\mathbf{E}}}$ representing the total electric field operator which satisfies the following set of Fourier-domain Maxwell equations

$$\boldsymbol{\nabla}\times\hat{\underline{\mathbf{E}}}(\mathbf{r},\omega) = ik\,\hat{\underline{\mathbf{H}}}(\mathbf{r},\omega), \tag{14}$$

$$\boldsymbol{\nabla}\times\hat{\underline{\mathbf{H}}}(\mathbf{r},\omega) = -ik\,\hat{\underline{\mathbf{E}}}(\mathbf{r},\omega) + \frac{4\pi}{c}\hat{\underline{\mathbf{I}}}(\mathbf{r},\omega). \tag{15}$$

Here, $\hat{\underline{\mathbf{H}}}$ stands for the magnetic field operator, $k = \omega/c$, and

$$\begin{aligned}\hat{\underline{\mathbf{I}}}(\mathbf{r},\omega) &= \int d\mathbf{R}\,\delta(\mathbf{r}-\mathbf{R})\,\hat{\underline{\mathbf{J}}}(\mathbf{R},\omega)\\ &= 2\hat{\underline{\mathbf{J}}}(R_{cn},\varphi,z,\omega)\,\delta(r-R_{cn})\,,\end{aligned} \tag{16}$$

is the exterior operator current density [with $\hat{\underline{\mathbf{J}}}(\mathbf{R},\omega)$ defined by Eq. (5)] associated with the presence of the CN.

From Eqs. (14)-(16) in view of Eq. (5), it follows that

$$\hat{\underline{\mathbf{E}}}(\mathbf{r},\omega) = i\frac{4\pi}{c}\,k\int d\mathbf{R}\,\mathbf{G}(\mathbf{r},\mathbf{R},\omega)\cdot\hat{\underline{\mathbf{J}}}(\mathbf{R},\omega) \tag{17}$$

[and $\hat{\underline{\mathbf{H}}} = (ik)^{-1}\boldsymbol{\nabla}\times\hat{\underline{\mathbf{E}}}$ accordingly], where $\mathbf{G}$ is the Green tensor of the classical electromagnetic field in the vicinity of the CN. The set of Eqs. (6)-(17) forms a closed electromagnetic field quantization formalism in the presence of dispersing and absorbing media which meets all the basic requirements of a standard quantum electrodynamics [16]. All information about medium (a CN in our case) is contained in the Green tensor $\mathbf{G}$ via the CN surface axial conductivity in Eq. (5). The Green tensor components satisfy the equation

$$\sum_{\alpha=r,\varphi,z}\left(\boldsymbol{\nabla}\times\boldsymbol{\nabla}\times - k^2\right)_{z\alpha}G_{\alpha z}(\mathbf{r},\mathbf{R},\omega) = \delta(\mathbf{r}-\mathbf{R}), \tag{18}$$

together with the radiation conditions at infinity and the boundary conditions on the CN surface. This tensor was derived and analysed in Ref. [10].

Assuming further that the atomic subsystem is sufficiently localized in space, so that the long-wavelength approximation applies, one can expand the field operators $\hat{\mathbf{A}}(\mathbf{r})$ and $\hat{\varphi}(\mathbf{r})$ in the Hamiltonian (6) around the atomic center of mass position $\mathbf{r}_A$ and only keep the leading non-vanishing terms of the expansions. Then, under the condition of the Coulomb gauge $[\hat{\mathbf{p}}_i, \hat{\mathbf{A}}] = 0$, one arrives at the approximate total Hamiltonian of the form

$$\hat{H} = \hat{H}_F + \hat{H}_A + \hat{H}^{(1)}_{AF} + \hat{H}^{(2)}_{AF}\,, \tag{19}$$

where

$$\hat{H}_F = \int_0^\infty d\omega\, \hbar\omega \int d\mathbf{R}\, \hat{f}^\dagger(\mathbf{R},\omega)\hat{f}(\mathbf{R},\omega)\,, \tag{20}$$

$$\hat{H}_A = \sum_i \frac{\hat{\mathbf{p}}^2}{2m_i} + \frac{1}{2}\sum_{i,j}\frac{q_i q_j}{|\mathbf{r}_i - \mathbf{r}_j|}\,, \tag{21}$$

$$\hat{H}^{(1)}_{AF} = -\sum_i \frac{q_i}{m_i c}\,\hat{\mathbf{p}}_i\cdot\hat{\mathbf{A}}(\mathbf{r}_A) + \hat{\mathbf{d}}\cdot\boldsymbol{\nabla}\hat{\varphi}(\mathbf{r}_A)\,, \tag{22}$$

$$\hat{H}^{(2)}_{AF} = \sum_i \frac{q_i^2}{2m_i c^2}\,\hat{\mathbf{A}}^2(\mathbf{r}_A) \tag{23}$$

are, respectively, the Hamiltonian of the vacuum electromagnetic field modified by the presence of the CN, the Hamiltonian of the atomic subsystem, and the electric dipole approximation for the Hamiltonian of the atom-field interaction (separated into two contributions according to their role in the vdW energy – see below) with $\hat{\mathbf{d}} = \sum_i q_i\hat{\mathbf{r}}_i$ being the electric dipole moment operator of the atomic subsystem.

B. The two-level approximation

Starting from Eqs. (19)-(23) and using Eqs. (9)-(13), (17) and (5), one obtains the following two-level approximation for the total Hamiltonian of the system (see Appendix A)

$$\hat{\mathcal{H}} = \hat{\mathcal{H}}_0 + \hat{\mathcal{H}}_{int}\,, \tag{24}$$

where the first term stands for the unperturbed Hamiltonian given by

$$\hat{\mathcal{H}}_0 = \hat{H}_F + \hat{\mathcal{H}}_A \tag{25}$$

with $\hat{H}_F$ being the Hamiltonian (20) of the CN modified field and

$$\hat{\mathcal{H}}_A = \frac{\hbar\tilde{\omega}_A}{2}\,\hat{\sigma}_z \tag{26}$$

representing the 'effective' unperturbed two-level atomic subsystem, and the second term stands for their interaction given by

$$\begin{aligned}\hat{\mathcal{H}}_{int} \;=\; &\int_0^\infty d\omega \int d\mathbf{R}\,[\,\mathrm{g}^{(+)}(\mathbf{r}_A,\mathbf{R},\omega)\,\hat{\sigma}^\dagger \\ &-\; \mathrm{g}^{(-)}(\mathbf{r}_A,\mathbf{R},\omega)\,\hat{\sigma}\,]\,\hat{f}(\mathbf{R},\omega) + \mathrm{h.c.}.\end{aligned} \tag{27}$$

Here, the Pauli operators

$$\begin{aligned}\hat{\sigma} = |l\rangle\langle u|\,,\;\; \hat{\sigma}^\dagger = |u\rangle\langle l|\,,\;\; \hat{\sigma}_z \;=\; |u\rangle\langle u| - |l\rangle\langle l|\,, \\ |u\rangle\langle u| + |l\rangle\langle l| \;=\; \hat{I}\,,\end{aligned} \tag{28}$$

describe electric dipole transitions between the two atomic states, upper $|u\rangle$ and lower $|l\rangle$, separated by the transition frequency ω_A. This 'bare' transition frequency is modified by the interaction (23) which, being independent of the atomic dipole moment, *does not* contribute to mixing the $|u\rangle$ and $|l\rangle$ states, giving rise, however, to the new *renormalized* transition frequency

$$\tilde{\omega}_A = \omega_A\left[1 - \frac{2}{(\hbar\omega_A)^2}\int_0^\infty d\omega \int d\mathbf{R}\,|\mathrm{g}^\perp(\mathbf{r}_A,\mathbf{R},\omega)|^2\right] \tag{29}$$

in the 'effective' atomic Hamiltonian (26). On the contrary, the interaction (22), being dipole moment dependent, mixes the $|u\rangle$ and $|l\rangle$ states, yielding the perturbation Hamiltonian (27) with the (dipole) interaction matrix elements of the form

$$\mathrm{g}^{(\pm)}(\mathbf{r}_A,\mathbf{R},\omega) = \mathrm{g}^\perp(\mathbf{r}_A,\mathbf{R},\omega) \pm \frac{\omega}{\omega_A}\,\mathrm{g}^\parallel(\mathbf{r}_A,\mathbf{R},\omega)\,, \tag{30}$$

where

$$\begin{aligned}&\mathrm{g}^{\perp(\parallel)}(\mathbf{r}_A,\mathbf{R},\omega) = \\ &-i\frac{4\omega_A}{c^2}\,d_z\sqrt{\pi\hbar\omega\,\mathrm{Re}\,\sigma_{zz}(\mathbf{R},\omega)}\;{}^{\perp(\parallel)}G_{zz}(\mathbf{r}_A,\mathbf{R},\omega)\end{aligned} \tag{31}$$

with

$${}^{\perp(\parallel)}G_{zz}(\mathbf{r}_A,\mathbf{R},\omega) = \int d\mathbf{r}\,\delta^{\perp(\parallel)}_{zz}(\mathbf{r}_A - \mathbf{r})\,G_{zz}(\mathbf{r},\mathbf{R},\omega) \tag{32}$$

being the field Green tensor zz-component transverse (longitudinal) with respect to the first variable. This is the only Green tensor component we have to take account of. All the other components can be safely be neglected, because our model neglects the azimuthal current and radial polarizability of the CN from the very outset.

The matrix elements (30) and (31) have the following properties (see Appendix B)

$$\int d\mathbf{R}\,|\mathrm{g}^{\perp(\parallel)}(\mathbf{r}_A,\mathbf{R},\omega)|^2 = \frac{(\hbar\omega_A)^2}{2\pi\omega^2}\,\Gamma_0(\omega)\,\xi^{\perp(\parallel)}(\mathbf{r}_A,\omega) \tag{33}$$

and

$$\begin{aligned}\int d\mathbf{R}\,|\mathrm{g}^{(\pm)}(\mathbf{r}_A,\mathbf{R},\omega)|^2 = &\frac{(\hbar\omega_A)^2}{2\pi\omega^2}\,\Gamma_0(\omega) \\ &\times\left[\xi^\perp(\mathbf{r}_A,\omega) + \left(\frac{\omega}{\omega_A}\right)^2\xi^\parallel(\mathbf{r}_A,\omega)\right].\end{aligned} \tag{34}$$

Here, $\xi^{\perp(\parallel)}(\mathbf{r}_A,\omega)$ is the transverse (longitudinal) *local* photonic DOS function defined by [10]

$$\xi^{\perp(\parallel)}(\mathbf{r}_A,\omega)=\frac{\Gamma^{\perp(\parallel)}(\mathbf{r}_A,\omega)}{\Gamma_0(\omega)}\,, \tag{35}$$

where

$$\Gamma^{\perp(\parallel)}(\mathbf{r}_A,\omega)=\frac{8\pi\omega^2}{\hbar c^2}\,d_z^2\,\mathrm{Im}^{\perp(\parallel)}G_{zz}^{\perp(\parallel)}(\mathbf{r}_A,\mathbf{r}_A,\omega) \tag{36}$$

is the transverse (longitudinal) atomic spontaneous decay rate near the CN with

$$^{\perp(\parallel)}G_{zz}^{\perp(\parallel)}(\mathbf{r}_A,\mathbf{r}_A,\omega)=\int d\mathbf{r}\,d\mathbf{r}'\,\delta_{zz}^{\perp(\parallel)}(\mathbf{r}_A-\mathbf{r}) \times G_{zz}(\mathbf{r},\mathbf{r}',\omega)\,\delta_{zz}^{\perp(\parallel)}(\mathbf{r}'-\mathbf{r}_A) \tag{37}$$

being the Green tensor zz-component transverse (longitudinal) with respect to both variables, and $\Gamma_0(\omega)$ is the same quantity in vacuum where [23]

$$\mathrm{Im}\,G_{zz}^0=\frac{\omega}{6\pi c}\,. \tag{38}$$

Note that the transverse and longitudinal imaginary Green tensor components in Eq. (36) can be written as

$$\mathrm{Im}^{\perp}G_{zz}^{\perp} = \mathrm{Im}\,G_{zz}^0+\mathrm{Im}^{\perp}\overline{G}_{zz}^{\perp}\,, \tag{39}$$

$$\mathrm{Im}^{\parallel}G_{zz}^{\parallel} = \mathrm{Im}^{\parallel}\overline{G}_{zz}^{\parallel} \tag{40}$$

with $^{\perp(\parallel)}\overline{G}_{zz}^{\perp(\parallel)}$ representing the "pure" CN contribution to the total imaginary Green tensor. The longitudinal imaginary Green tensor in Eq. (40) is totally contributed by a (longitudinal) CN static polarization field and, therefore, does not contain the vacuum term which is the transverse one by its definition as there are no polarization Coulomb sources in vacuum. Thus, Eq. (35) may, in view of Eqs. (36)–(40), be rewritten in the form

$$\xi^{\perp}(\mathbf{r}_A,\omega) = 1+\overline{\xi}^{\perp}(\mathbf{r}_A,\omega)\,, \tag{41}$$

$$\xi^{\parallel}(\mathbf{r}_A,\omega) = \overline{\xi}^{\parallel}(\mathbf{r}_A,\omega)\,, \tag{42}$$

where the $\mathbf{r}_A$-dependent terms come totally from the presence of the CN.

Eqs. (24)-(31) represent the total secondly quantized Hamiltonian of an atomic system interacting with the electromagnetic field in the vicinity of the carbon nanotube. In deriving this Hamiltonian, there were only two standard approximations done. They are the electric dipole approximation and the two-level approximation. The rotating wave approximation commonly used was not applied, and the (diamagnetic) $\hat{\mathbf{A}}^2$-term of the atom-field interaction [Eq. (23)] was not neglected. The latter two approximations are justified in analyzing an atomic state evolution due to *real* dipole transitions to the nearest states [24], described for two-level systems by the $\mathrm{g}^{(+)}$-terms of the Hamiltonian (27). They are, however, inappropriate in calculating the energy, where the initial energy level is being shifted due to the perturbation caused by *virtual* dipole transitions via intermediate atomic states, so that the system always remains in the initial state and the terms neglected contribute to the level shift to the same order of magnitude. For two-level systems, this is described by $\mathrm{g}^{(-)}$-terms of the Hamiltonian (27) (usually neglected within the rotating wave approximation) together with the atomic transition frequency (29) renormalized due to the (usually discarded) $\hat{\mathbf{A}}^2$-term of the atom-field interaction.

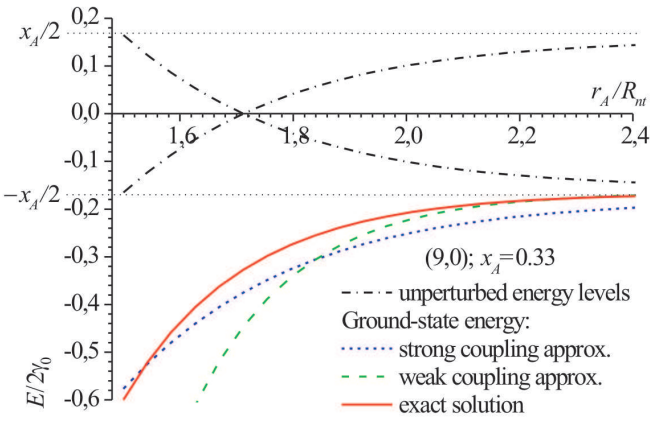

FIG. 2: (Color online) Dimensionless unperturbed energy levels [given by the Hamiltonian (25)] and total ground-state energy [given by Eqs. (46)-(50)] as functions of the atomic position for the two-level atom outside the (9,0) CN.

C. The van der Waals energy

The Hamiltonian (24)-(27) is a starting point for the atom-nanotube vdW energy calculation. Supposing the two-level atom to be in the ground state, the vdW energy is nothing but the $\mathbf{r}_A$-dependent contribution to the ground-state eigenvalue of this Hamiltonian. Important is that the unperturbed atomic subsystem is now described by the Hamiltonian (26) with the renormalized transition frequency (29) which is represented in terms of the local photonic DOS (35) as

$$\tilde{\omega}_A=\omega_A\left[1-\frac{1}{\pi}\int_0^\infty d\omega\frac{\Gamma_0(\omega)}{\omega^2}\,\xi^{\perp}(\mathbf{r}_A,\omega)\right]. \tag{43}$$

As is seen from Eq. (43), the transition frequency $\tilde{\omega}_A$ decreases with increasing the transverse local photonic DOS $\xi^{\perp}(\mathbf{r}_A,\omega)$, i.e. when the atom approaches the CN surface [10], thereby bringing the unperturbed atomic levels together, or even making them degenerated if $\xi^{\perp}(\mathbf{r}_A,\omega)$ is large enough (see a typical example in Fig. 2). If one uses the standard perturbation theory, this would yield the divergence of high-order corrections to the vdW energy at small atom-CN-surface distances because of the small energy denominators in the corresponding power-series expansions. To account for a possible degeneracy of

the unperturbed atomic levels in a correct way, one has to use the perturbation theory for degenerated atomic levels (see, e.g., [14]). In so doing, one has to take the upper state degeneracy into account of the whole system with respect to $\mathbf{R}$, so that the ground-state wave function of the whole system should be represented as a coherent mixture of the lower and upper states of the form

$$|\psi\rangle = C_l\,|l\rangle|\{0\}\rangle + \int_0^\infty d\omega \int d\mathbf{R}\, C_u(\mathbf{R},\omega)\,|u\rangle|\{1(\mathbf{R},\omega)\}\rangle, \tag{44}$$

where $|\{0\}\rangle$ is the vacuum state of the field subsystem, $|\{1(\mathbf{R},\omega)\}\rangle$ is its single-quantum excited state, C_l and $C_u(\mathbf{R},\omega)$ are unknown mixing coefficients of the lower and upper states of the *whole* system.

The total energy E of the ground state is now given by the solution of a secular equation obtained by applying the Hamiltonian (24)-(27) to the wave function (44). This yields the integral equation

$$E = -\frac{\hbar\tilde{\omega}_A}{2} - \int_0^\infty d\omega \int d\mathbf{R}\, \frac{|\mathrm{g}^{(-)}(\mathbf{r}_A,\mathbf{R},\omega)|^2}{\hbar\omega + \dfrac{\hbar\tilde{\omega}_A}{2} - E}\,, \tag{45}$$

which the ground-state-atom vdW energy $E_{vw}(\mathbf{r}_A)$ is determined from by means of an obvious relation

$$E = -\frac{\hbar\omega_A}{2} + E_{vw}(\mathbf{r}_A)\,, \tag{46}$$

with the first term representing the 'bare' (non-interacting) two-level atom in the ground-state. Using dimensionless variables

$$\varepsilon_{vw}(\mathbf{r}_A) = \frac{E_{vw}(\mathbf{r}_A)}{2\gamma_0}\,,\quad \tilde{\Gamma}_0(x) = \frac{\hbar\Gamma_0(x)}{2\gamma_0}\,,\quad x = \frac{\hbar\omega}{2\gamma_0} \tag{47}$$

with $\gamma_0 = 2.7$ eV being the carbon nearest neighbor hopping integral appearing in the CN surface axial conductivity σ_{zz} in Eq. (5), and Eqs. (34), (41)–(43), one can represent the dimensionless vdW energy $\varepsilon_{vw}(\mathbf{r}_A)$ in terms of the transverse and longitudinal distance-dependent photonic DOS's in the vicinity of the nanotube. In so doing, one arrives at the integral equation of the form

$$\varepsilon_{vw}(\mathbf{r}_A) = \frac{x_A}{2\pi}\int_0^\infty dx \frac{\tilde{\Gamma}_0(x)}{x^2}\,\overline{\xi}^{\,\perp}(\mathbf{r}_A,x) - \frac{x_A^2}{2\pi}\int_0^\infty dx \frac{\tilde{\Gamma}_0(x)}{x^2}\,\frac{\overline{\xi}^{\,\perp}(\mathbf{r}_A,x) + \left(\dfrac{x}{x_A}\right)^2\overline{\xi}^{\,\parallel}(\mathbf{r}_A,x)}{x + x_A\left[1 - \dfrac{1}{2\pi}\displaystyle\int_0^\infty dx \frac{\tilde{\Gamma}_0(x)}{x^2}\,\overline{\xi}^{\,\perp}(\mathbf{r}_A,x)\right] - \varepsilon_{vw}(\mathbf{r}_A)} \tag{48}$$

with $\overline{\xi}^{\,\perp(\parallel)}(\mathbf{r}_A,x)$ given for $r_A > R_{cn}$ by (Appendix B)

$$\overline{\xi}^{\,\perp}(\mathbf{r}_A,x) \;=\; \frac{3}{\pi}\,\mathrm{Im}\sum_{p=-\infty}^{\infty}\int_C \frac{dy\, s(R_{cn},x)v(y)^4 I_p^2[v(y)u(R_{cn})x]K_p^2[v(y)u(r_A)x]}{1 + s(R_{cn},x)v(y)^2 I_p[v(y)u(R_{cn})x]K_p[v(y)u(R_{cn})x]}\,, \tag{49}$$

$$\overline{\xi}^{\,\parallel}(\mathbf{r}_A,x) \;=\; \frac{3}{\pi}\,\mathrm{Im}\sum_{p=-\infty}^{\infty}\int_C \frac{dy\, s(R_{cn},x)y^2v(y)^2 I_p^2[v(y)u(R_{cn})x]K_p^2[v(y)u(r_A)x]}{1 + s(R_{cn},x)v(y)^2 I_p[v(y)u(R_{cn})x]K_p[v(y)u(R_{cn})x]}\,, \tag{50}$$

where I_p and K_p are the modified cylindric Bessel functions, $v(y) = \sqrt{y^2-1}$, $u(r) = 2\gamma_0 r/\hbar c$, and $s(R_{cn},x) = 2i\alpha u(R_{cn})x\overline{\sigma}_{zz}(R_{cn},x)$ with $\overline{\sigma}_{zz} = 2\pi\hbar\sigma_{zz}/e^2$ being the dimensionless CN surface conductivity per unit length and $\alpha = e^2/\hbar c = 1/137$ representing the fine-structure constant. The integration contour C goes along the real axis of the complex plane and envelopes the branch points $y = \pm 1$ of the function $v(y)$ in the integrands from below and from above, respectively. For $r_A < R_{cn}$, Eqs. (49) and (50) are modified by a simple replacement $r_A \leftrightarrow R_{cn}$ in the Bessel function arguments in the numerators of the integrands.

III. QUALITATIVE ANALYSIS

Eqs. (48)-(50) describe the ground-state-atom vdW energy near an infinitely long single-wall carbon nanotube in terms of the local (distance-dependent) photonic DOS. Eq. (48) is universal in the sense that it covers both strong and weak atom-field coupling regimes defined as those violating and non-violating, respectively, the applicability domain of the conventional stationary perturbation theory [40].

1. Weak coupling regime

If, when the atom is faraway from the CN, the local photonic DOS $\overline{\xi}^{\perp}(\mathbf{r}_A, x)$ is such small that

$$\frac{1}{2\pi}\int_0^\infty dx \frac{\tilde{\Gamma}_0(x)}{x^2}\,\overline{\xi}^{\perp}(\mathbf{r}_A, x) \ll 1 \tag{51}$$

and

$$\varepsilon_{vw}(\mathbf{r}_A) \sim 0\,, \tag{52}$$

then Eq. (48) yields a well-known perturbation theory result (see, e.g., [11]) of the form

$$\varepsilon_{vw}(\mathbf{r}_A) \approx \frac{x_A}{2\pi}\int_0^\infty dx \frac{\tilde{\Gamma}_0(x)}{x^2}\,\overline{\xi}^{\perp}(\mathbf{r}_A, x)$$
$$-\frac{x_A^2}{2\pi}\int_0^\infty dx \frac{\tilde{\Gamma}_0(x)}{x^2}\,\frac{\overline{\xi}^{\perp}(\mathbf{r}_A, x) + \left(\dfrac{x}{x_A}\right)^2 \overline{\xi}^{\parallel}(\mathbf{r}_A, x)}{x + x_A}\,, \tag{53}$$

where the first term comes from the unperturbed Hamiltonian (25), (26) and the second one is the second order correction due to the perturbation (27). This can be equivalently rewritten in the form

$$\varepsilon_{vw}(\mathbf{r}_A) \;\approx\; \frac{x_A}{2\pi}\int_0^\infty dx \frac{\tilde{\Gamma}_0(x)}{x(x + x_A)}$$
$$\times\; \left[\overline{\xi}^{\perp}(\mathbf{r}_A, x) - \frac{x}{x_A}\,\overline{\xi}^{\parallel}(\mathbf{r}_A, x)\right], \tag{54}$$

from which, in view of Eqs. (49), (50) and basic properties of the modified cylindric Bessel functions [26], one can immediately come to an interesting conclusion. Namely, if the atom is fixed outside (inside) the CN in a way that the weak atom-field coupling regime is realized, i.e. far enough from the CN surface, then the modulus of the atom-nanotube vdW energy increases (decreases) with the CN radius. The conclusion is physically clear as the effective atom-nanotube interaction area is larger (smaller) for larger-radius nanotubes when the atom is outside (inside) the CN. Important, however, is that this obvious conclusion is, strictly speaking, only valid in the weak atom-field coupling regime for the outside atomic position, while for the inside atomic position it represents a general effect of the effective interaction area reduction with lowering the CN surface curvature.

In the large CN radius limit, Eq. (54) along with Eqs. (49) and (50) can be shown to reproduce a well-known Casimir-Polder result [27] for an atom near an infinitely conducting plane (see Appendix C).

2. Strong coupling regime

When the atom is close enough to the CN surface, the local photonic DOS $\overline{\xi}^{\perp}(\mathbf{r}_A, x)$ is large, so that one might expect the condition

$$\frac{1}{2\pi}\int_0^\infty dx \frac{\tilde{\Gamma}_0(x)}{x^2}\,\overline{\xi}^{\perp}(\mathbf{r}_A, x) \sim 1 \tag{55}$$

to hold true. Under this condition, Eq. (48) reduces to an integral equation of the form

$$\varepsilon_{vw}(\mathbf{r}_A) \approx \frac{x_A}{2\pi}\int_0^\infty dx \frac{\tilde{\Gamma}_0(x)}{x^2}\,\overline{\xi}^{\perp}(\mathbf{r}_A, x)$$
$$-\frac{x_A^2}{2\pi}\int_0^\infty dx \frac{\tilde{\Gamma}_0(x)}{x^2}\,\frac{\overline{\xi}^{\perp}(\mathbf{r}_A, x) + \left(\dfrac{x}{x_A}\right)^2 \overline{\xi}^{\parallel}(\mathbf{r}_A, x)}{x - \varepsilon_{vw}(\mathbf{r}_A)} \tag{56}$$

valid in the strong atom-field coupling regime.

Eq. (55) corresponds to the *inverted* unperturbed atomic levels described by the Hamiltonian (26) with $\tilde{\omega}_A$ given by Eq. (43) (see Fig. 2 as an example). The levels are degenerated when the left-hand side of Eq. (55) is exactly 0.5. A noteworthy point is that if one used the weak coupling approximation of Eq. (48) for the atom close to the CN surface where Eq. (51) is not satisfied and Eq. (55) holds true instead, then the result would be divergent at the lower limit of integration. To avoid this fact, one has to use either strong coupling approximation (56) or the exact equation (48) to calculate the vdW energy of the atom close to the nanotube surface.

IV. NUMERICAL RESULTS AND DISCUSSION

Using Eqs. (46)-(50), we have simulated the total ground state energy of the whole system "two-level atom + CN-modified vacuum electromagnetic field" and the vdW energy of the two-level atom nearby metallic and semiconducting carbon nanotubes of different radii. The dimensionless free-space spontaneous decay rate in Eq. (48) was approximated by the expression $\tilde{\Gamma}_0(x) \approx 4\alpha^3 x^3/3x_A^2$ ($\alpha = 1/137$ is the fine-structure constant) valid for atomic systems with Coulomb interaction [14].

Figure 2 shows the dimensionless ground state energy level of the whole system [given by the corresponding eigenvalue of the the total Hamiltonian (19) and represented by Eqs. (46)-(50)] and two dimensionless energy levels of the unperturbed Hamiltonian (25), (26) as functions of the atomic position outside the (9,0) CN. As the atom approaches the CN surface, its unperturbed levels come together, then get degenerated and even inverted at a very small atom-surface distance. In so doing, the weak coupling approximation for the ground state energy [given by Eqs. (46), (47), (54) and (49), (50)] diverges near the surface, whereas the strong coupling approximation [Eqs. (46), (47), (56) and (49), (50)] yields a finite result. The exact solution reproduces the weak-coupling approximation at large and the strong-coupling approximation at short atom-surface distances, respectively.

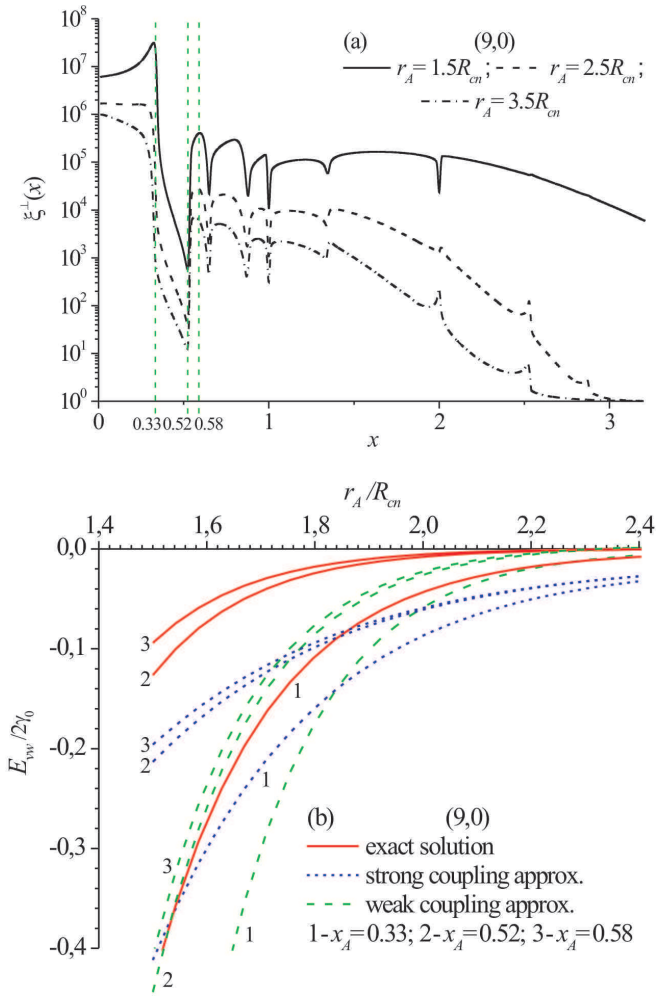

FIG. 3: (Color online) Transverse local photonic DOS's (a) and ground-state vdW energies (b) as functions of the atomic position for the two-level atom outside the (9,0) CN. The 'bare' atomic transition frequencies are indicated by dashed lines in Fig. 3(a).

The degeneracy of the unperturbed atomic levels is the consequence of the transverse local photonic DOS increase [see Eq. (43)] as the atom approaches the CN surface. A typical example is shown in Fig. 3 (a) for the atom outside the (9,0) CN. The transverse DOS function is seen to increase with decreasing the atom-CN-surface distance, representing the atom-field coupling strength enhancement with surface photonic modes of the nanotube as the atom approaches the nanotube surface [8, 10]. The vertical dashed lines indicate the 'bare' atomic transition frequencies x_A for which the vdW energies shown in Fig. 3 (b) were calculated. Some of them are the positions of peaks, the others are the positions of dips of the local photonic DOS. They are typical for some rear-earth ions such as Europium, or for heavy hydrogen-like atoms such as Caesium (supposed to be non-ionized near the CN). For example [28], for a well-known two-level dipole transition $^7F_2 \leftrightarrow {}^5D_0$ of Europium at $\lambda = 615$ nm one has $x_A \approx 0.37$, whereas for Caesium one obtains from its first ionization potential [29] the estimate $x_A \approx 3.89\,\mathrm{eV} \times 3/4 \times (2\gamma_0)^{-1} \approx 0.5$ (the factor 3/4 comes from the Lyman series of Hydrogen), or less for highly excited Rydberg states.

Figure 3 (b) shows the vdW energies of the atom outside the (9,0) CN for three different 'bare' atomic transition frequencies [indicated by vertical dashed lines in Fig. 3 (a)]. Here, exact numerical solutions of Eqs. (48)-(50) are compared with those obtained within the weak coupling approximation (54), (49), (50) and within the strong coupling approximation (56), (49), (50). At small atom-CN-surface distances, the exact solutions are seen to be fairly well reproduced by those obtained in the strong coupling approximation, clearly indicating the strong atom-field coupling regime in a close vicinity of the nanotube surface. The deviation from the strong coupling approximation increases with transition frequency x_A,

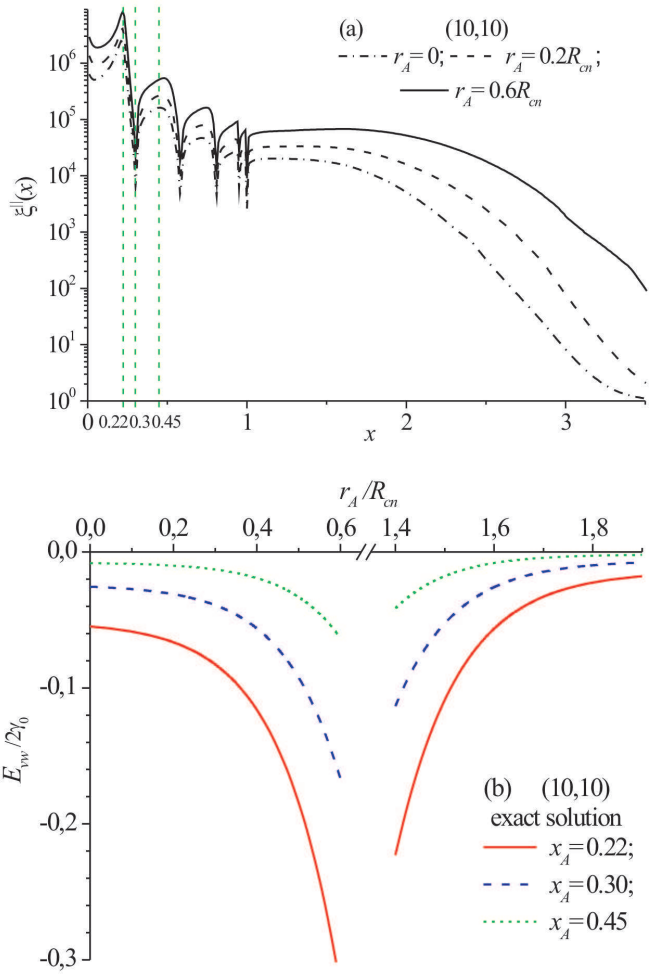

FIG. 4: (Color online) Longitudinal local photonic DOS's (a) and ground-state vdW energies (b) as functions of the atomic position for the two-level atom nearby the (10,10) CN. The 'bare' atomic transition frequencies are indicated by dashed lines in Fig. 4(a).

that is easily explicable since the degeneracy condition (55) of the unperturbed atomic levels is more difficult to reach for larger inter-level separations. As the atom moves away from the CN surface, the exact solutions deviate from the strong coupling solutions and approach those given by the weak coupling approximation, indicating the reduction of the atom-field coupling strength with raising the atom-surface distance. The weak-coupling solutions are seen to be divergent close to the nanotube surface as it should be because of the degeneracy of the unperturbed atomic levels in this region.

Figure 4 (a) shows the longitudinal local photonic DOS's for the atom inside the (10,10) CN at three representative distances from the nanotube wall. As the atom approaches the wall, the longitudinal DOS function increases in a similar way as the transverse DOS function does in Fig. 3 (a). The vertical dashed lines indicate the 'bare' atomic transition frequencies for which the atomic vdW energies in Fig. 4 (b) were calculated. Figure 4 (b) represents the exact solutions of Eq. (48) for atom inside and outside the (10,10) CN. When the atom is inside, the vdW energies are seen to be in general lower than those for the atom outside the CN. This may be attributed to the fact that, due to the nanotube curvature, the effective interaction area between the atom and the CN surface is larger when the atom is inside rather than when it is outside the CN. This, in turn, indicates that encapsulation of doped atoms into the nanotube is energetically more favorable than their outside adsorption by the nanotube surface — the effect observed experimentally in Ref. [5].

Comparing Fig. 3 (b) with Fig. 4 (b) for the outside atomic position, one can see that, if the atom-CN-surface distance is so large that the weak-coupling approximation is good, then for the same distance and approximately the same atomic transition frequency $x_A \approx 0.3$ the vdW energy near the (10,10) nanotube ($R_{cn} = 6.78$ Å) is lower than that near the (9,0) nanotube ($R_{cn} = 3.52$ Å). This is in agreement with the qualitative predictions formulated above in analyzing the weak coupling regime. In the present case, the effective atom-CN-surface interaction area is larger for the atom outside the larger-radius (10,10) nanotube, thereby explaining the effect. Obviously, one should expect an opposite effect for the inside atomic position. Experimentally, the heat of absorbtion of Krypton, to take an example, has been shown to be larger for graphite (0.17 eV/atom) than for multiwall nanotubes (0.12 eV/atom) [30], in agreement with our theoretical predictions.

A similar tendency is demonstrated in Fig 5. Here, the vdW energies calculated from Eqs. (48)-(50) are represented for the atom positioned at a fixed distance from the nanotube wall [chosen to be equal to the radius of the (9,0) CN] inside and outside the "zigzag" $(m, 0)$ CNs of increasing radius $R_{cn} = m\,(a\sqrt{3}/2\pi)$ (a=1.42 Å is the CN interatomic distance). When the atom is inside, the energy absolute value goes down with R_{cn}, representing a general tendency of the effective interaction area reduction with lowering the CN surface curvature. When the

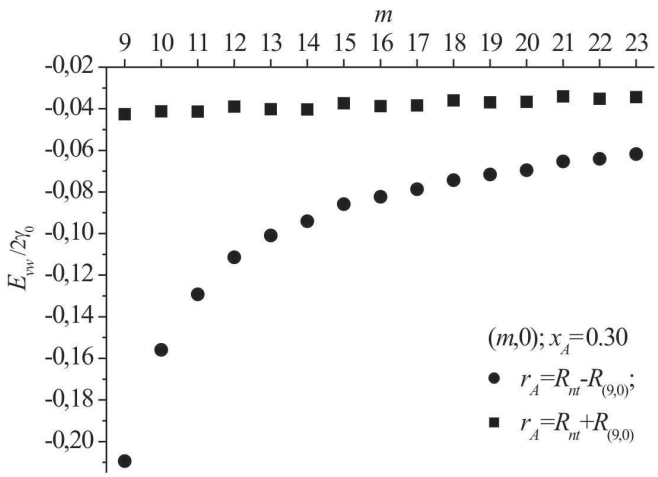

FIG. 5: Ground-state van der Waals energy of the two-level atom positioned at a fixed atom-surface distance [equal to the radius of the (9,0) CN] inside and outside "zigzag" $(m, 0)$ CNs of different radii, as a function of the nanotube index m.

atom is outside, the effect would be the opposite one if the atom were weakly coupled to the field, thus indicating that the atom-field coupling regime is not actually weak for the distance chosen. In general, the inside and outside vdW energies approach each other with R_{cn} as it should be since the two atomic positions become equivalent in the plane limit where $R_{cn} \to \infty$. Interesting is also the fact that the vdW energies of the atom outside the metallic nanotubes (m is divisible by 3) are on average a little bit smaller than those for the atom outside semiconducting ones. This is certainly the property related to the difference in the conductivities of metallic and semiconducting "zigzag" nanotubes.

V. CONCLUSIONS

Recently, a theory of atomic spontaneous decay near CNs was developed [8, 9, 10]. The theory has brought out fascinating peculiarities of the vacuum-field interactions in atomically doped CNs. In particular [9, 10], if the atom is close enough to the CN surface and the atomic transition frequency is in the vicinity of a resonance of the photonic DOS, the atomic spontaneous decay dynamics exhibits vacuum-field Rabi oscillations. This is a principal signature of strong coupling of the excited atomic state to vacuum surface photonic modes in the CN. Such a strongly coupled atomic state is nothing but a 'quasi-1D cavity polariton' similar to quasi-0D excitonic (electronic) polaritons in quantum dot microcavities widely discussed in the literature [31, 32, 33]. The study of such phenomena was started awhile ago in atomic physics [34] and still attracts a lot of interest especially in connection with research on quantum computation [35].

Obviously, the stability of quasi-1D atomic polaritons in CNs is mainly determined by the atom-nanotube van

der Waals interaction. This interaction, however, originates from *strong* atom-field coupling and, therefore, cannot be correctly described in terms of vacuum-QED-based (weak-coupling) vdW interaction models as well as in terms of those based upon the linear response theory. In the present paper, we have developed a simple quantum mechanical approach to the ground-state vdW energy calculation of a (two-level) atomic system near a CN. The approach is based upon the perturbation theory for degenerated atomic levels, thus accounting for both weak and strong atom-field coupling and thereby covering the vdW interactions of the ground-state quasi-1D atomic polaritons in CNs. Within the framework of this approach, the vdW energy is described by the integral equation represented in terms of the local photonic DOS. By solving this equation numerically, we have demonstrated the inapplicability of weak-coupling-based vdW interaction models in a close vicinity of the nanotube surface where the local photonic DOS effectively increases, giving rise to an atom-field coupling enhancement followed by the degeneracy of the unperturbed atomic levels due to the diamagnetic interaction term.

The fundamental conclusion above is supplemented by those important for various applications of atomically doped CNs in modern nanotechnology. In particular, we have studied CN surface curvature effects on the atom-nanotube vdW interactions and have shown that an inside encapsulation of doped atoms into the nanotube is energetically more favorable than their outside adsorption by the nanotube surface, in agreement with the experimental observations reported in Ref. [5]. Moreover, if the atom is fixed outside the CN in a way that the weak atom-field coupling regime is realized, i.e. far enough from the CN surface, then the modulus of the atom-nanotube vdW energy increases with the CN radius because the effective atom-nanotube interaction area is larger for larger-radius nanotubes in this case. For inside atomic position, the modulus of the atom-nanotube vdW energy decreases with the CN radius, representing a general effect of the effective interaction area reduction with lowering the CN surface curvature.

A further intriguing extension of the present work could be the vdW interactions of excited atomic states where, even in the weak atom-field-coupling regime and in the simplest case of an atom near a planar semi-infinite medium, very interesting peculiarities (e.g., oscillatory behavior) were recently shown to exist [12].

Acknowledgments

Discussions with Prof. D.-G.Welsch and Dr. S.Y.Buhmann are gratefully acknowledged. The work was done in part within the framework of the Belgian PAI-P5/01 project during the stay of one of the authors (I.B.) in the University of Namur, Belgium. I.B. thanks the Belgian OSTC.

APPENDIX A: THE TWO-LEVEL APPROXIMATION

In this Appendix, we rewrite the Hamiltonian (19)-(23) in terms of a two-level atomic model [24]. Within the framework of this model, the spectrum of the atomic Hamiltonian (21) is approximated by the two eigenstates, upper $|u\rangle$ and lower $|l\rangle$, with the energies $\hbar\omega_u$ and $\hbar\omega_l$, respectively. One has then

$$\hat{H}_A \approx \hbar\omega_u |u\rangle\langle u| + \hbar\omega_l |l\rangle\langle l| \tag{A1}$$

with a completeness relation

$$|u\rangle\langle u| + |l\rangle\langle l| = \hat{I}. \tag{A2}$$

Subtracting a constant term $(\hbar/2)(\omega_u + \omega_l)\hat{I}$ from the Hamiltonian (A1) and thereby placing the energy zero in the middle between the two energy levels, one arrives at the 'bare' two-level atomic Hamiltonian of the form

$$\hat{H}_A = \frac{\hbar\omega_A}{2}\,\hat{\sigma}_z \tag{A3}$$

with $\hat{\sigma}_z = |u\rangle\langle u| - |l\rangle\langle l|$ and $\omega_A = \omega_u - \omega_l$ being the 'bare' atomic transition frequency.

In terms of such a two-level scheme, the atomic dipole moment operator $\hat{\mathbf{d}}$ has the matrix elements $\langle u|\hat{\mathbf{d}}|l\rangle = \langle l|\hat{\mathbf{d}}|u\rangle = \mathbf{d}$ and $\langle u|\hat{\mathbf{d}}|u\rangle = \langle l|\hat{\mathbf{d}}|l\rangle = 0$. Keeping this and the completeness relation (A2) in mind, the interaction Hamiltonians (22) and (23) can be rewritten as follows.

For the interaction (22), using Eqs. (9) and (10) and a well-known quantum mechanical operator equality

$$(\hat{\mathbf{p}}_i)_\alpha = m_i \frac{d}{dt}(\hat{\mathbf{r}}_i)_\alpha = \frac{m_i}{i\hbar}\left[(\hat{\mathbf{r}}_i)_\alpha, \hat{H}_A\right], \tag{A4}$$

where the Latin and Greek indexes enumerate particles in the atom and vector components, respectively, and $\hat{H}_A$ is given by Eq. (A3), one has

$$\begin{aligned}\hat{H}^{(1)}_{AF} &= (\hat{\sigma} - \hat{\sigma}^\dagger)\,\mathbf{d}\cdot\left[\int_0^\infty d\omega \frac{\omega_A}{\omega}\,\underline{\hat{\mathbf{E}}}^{\perp}(\mathbf{r}_A,\omega) - \text{h.c.}\right] \\ &- (\hat{\sigma} + \hat{\sigma}^\dagger)\,\mathbf{d}\cdot\left[\int_0^\infty d\omega\,\underline{\hat{\mathbf{E}}}^{\parallel}(\mathbf{r}_A,\omega) + \text{h.c.}\right],\end{aligned} \tag{A5}$$

with $\hat{\sigma} = |l\rangle\langle u|$ and $\hat{\sigma}^\dagger = |u\rangle\langle l|$. Using further Eqs. (11), (17) and (5) and assuming the longitudinal (along the CN axis) atomic dipole orientation due to the dominant axial polarizability of the nanotube [18, 19, 20, 21], one arrives at the secondly quantized interaction Hamiltonian (27) with the interaction matrix elements (30) and (31).

For the interaction (23), one may proceed as follows

$$\begin{aligned}\hat{H}^{(2)}_{AF} &= \sum_{i,j}\sum_{\alpha,\beta}\frac{q_i q_j}{2m_i c^2}\,\delta_{ij}\delta_{\alpha\beta}\hat{A}_\alpha(\mathbf{r}_A)\hat{A}_\beta(\mathbf{r}_A) \\ &= \frac{i}{2\hbar c^2}\sum_{i,\alpha,\beta}\frac{q_i}{m_i}[(\hat{\mathbf{p}}_i)_\alpha, \hat{d}_\beta]\hat{A}_\alpha(\mathbf{r}_A)\hat{A}_\beta(\mathbf{r}_A),\end{aligned} \tag{A6}$$

where the product of the two Kronecker-symbols in the first line is represented in terms of the 'coordinate-momentum' commutator as

$$\delta_{ij}\delta_{\alpha\beta} = \frac{i}{\hbar}\,[(\hat{\mathbf{p}}_i)_\alpha, (\hat{\mathbf{r}}_j)_\beta].$$

Using Eq. (A4) for the momentum operator components and the completeness relation (A2), one arrives at

$$\hat{H}^{(2)}_{AF} = -\frac{\omega_A}{\hbar c^2}\,\hat{\sigma}_z\Big[\mathbf{d}\cdot\hat{\mathbf{A}}(\mathbf{r}_A)\Big]^2 \tag{A7}$$

which, upon substituting Eq. (9) for the vector potential operator, becomes

$$-\frac{\hat{\sigma}_z}{\hbar\omega_A}\sum_{\alpha,\beta} d_\alpha d_\beta \left\{\int_0^\infty d\omega \frac{\omega_A}{i\omega}\int_0^\infty d\omega' \frac{\omega_A}{i\omega'}\,\underline{\hat{E}}^{\perp}_\alpha(\mathbf{r}_A,\omega)\,\underline{\hat{E}}^{\perp}_\beta(\mathbf{r}_A,\omega') - \int_0^\infty d\omega \frac{\omega_A}{i\omega}\int_0^\infty d\omega' \frac{\omega_A}{i\omega'}\,\underline{\hat{E}}^{\perp}_\alpha(\mathbf{r}_A,\omega)\Big[\underline{\hat{E}}^{\perp}_\beta(\mathbf{r}_A,\omega')\Big]^\dagger + \text{h.c.}\right\}.$$

The four items here can, in view of Eqs. (11), (17) and (5), be classified as follows. The first item and its hermitian conjugate describe the processes with simultaneous annihilation and creation of *two* photons (two-photon transitions). They may be safely neglected if the field intensity is low enough that, we believe, is the case for the vacuum electromagnetic field we deal with in considering the vdW interactions. Furthermore, keeping them in the Hamiltonian $\hat{H}^{(2)}_{AF}$ is meaningless as the Hamiltonian $\hat{H}^{(1)}_{AF}$ is nothing but a dipole approximation which, by its definition, neglects two-photon transitions. The second item and its hermitian conjugate are combined together by using bosonic commutation relations (2) to give in terms of the bosonic field operators and the transverse dipole interaction matrix element (31) the expression

$$-\frac{\hat{\sigma}_z}{\hbar\omega_A}\int_0^\infty d\omega \int d\mathbf{R}\,|\mathrm{g}^{\perp}(\mathbf{r}_A,\mathbf{R},\omega)|^2 - \frac{2\hat{\sigma}_z}{\hbar\omega_A}\int_0^\infty d\omega\,d\omega' \int d\mathbf{R}\,d\mathbf{R}'\,\big[\mathrm{g}^{\perp}(\mathbf{r}_A,\mathbf{R},\omega)\big]^*\mathrm{g}^{\perp}(\mathbf{r}_A,\mathbf{R}',\omega')f^\dagger(\mathbf{R},\omega)f(\mathbf{R}',\omega'),$$

where the second term is nothing but a two-photon correction to the dipole interaction (27), that can be easily seen by noting that $\hat{\sigma}_z = \hat{\sigma}^\dagger\hat{\sigma} - \hat{\sigma}\hat{\sigma}^\dagger$. This correction must be neglected for the reasons just discussed, so that finally one arrives at

$$\hat{H}^{(2)}_{AF} \approx -\frac{\hat{\sigma}_z}{\hbar\omega_A}\int_0^\infty d\omega \int d\mathbf{R}\,|\mathrm{g}^{\perp}(\mathbf{r}_A,\mathbf{R},\omega)|^2. \tag{A8}$$

Eq. (A8) can now be combined with the 'bare' atomic Hamiltonian (A3) to yield the 'effective' unperturbed atomic Hamiltonian (26) with the renormalized atomic transition frequency given by Eq. (29).

Thus, we have proved that the Hamiltonian (19)-(23), being approximated in terms of the two-level atomic model, is represented by the Hamiltonian (24)-(27).

APPENDIX B: THE TRANSVERSE AND LONGITUDINAL LOCAL PHOTONIC DOS

We start with Eq. (18) for the Green tensor of the electromagnetic subsystem. This equation is a direct consequence of the equation

$$\sum_{\alpha=r,\varphi,z}\big(\boldsymbol{\nabla}\times\boldsymbol{\nabla}\times - k^2\big)_{z\alpha}\,\underline{\hat{E}}_\alpha(\mathbf{r},\omega) = i\frac{4\pi}{c}\,k\,\underline{\hat{I}}_z(\mathbf{r},\omega) \tag{B1}$$

obtained by substituting the magnetic field operator from Eq. (14) into Eq. (15). On the other hand, under the condition of the Coulomb gauge (see, e.g., [36]), one has

$$\underline{\hat{\mathbf{E}}}(\mathbf{r},\omega) = \underline{\hat{\mathbf{E}}}^{\perp}(\mathbf{r},\omega) + \underline{\hat{\mathbf{E}}}^{\parallel}(\mathbf{r},\omega) \tag{B2}$$

with [compare with Eqs. (9) and (10)]

$$\underline{\hat{\mathbf{E}}}^{\perp}(\mathbf{r},\omega) = ik\underline{\hat{\mathbf{A}}}(\mathbf{r},\omega)\,, \tag{B3}$$

where

$$\boldsymbol{\nabla}\cdot\underline{\hat{\mathbf{A}}}(\mathbf{r},\omega) = 0\,, \tag{B4}$$

and

$$\underline{\hat{\mathbf{E}}}^{\parallel}(\mathbf{r},\omega) = -\boldsymbol{\nabla}\varphi(\mathbf{r},\omega)\,. \tag{B5}$$

From Eqs. (B1)–(B5), in view of Eq. (11) and (17), one obtains the following equation for the Green tensor components

$$\sum_{\alpha=r,\varphi,z}\big(\boldsymbol{\nabla}\times\boldsymbol{\nabla}\times - k^2\big)_{z\alpha}\Big[{}^{\perp}G_{\alpha z}(\mathbf{r},\mathbf{R},\omega) + {}^{\parallel}G_{\alpha z}(\mathbf{r},\mathbf{R},\omega)\Big] = \delta(\mathbf{r}-\mathbf{R}) \tag{B6}$$

with additional constraints

$$\sum_{\alpha=r,\varphi,z}\nabla_\alpha\,{}^{\perp}G_{\alpha z}(\mathbf{r},\mathbf{R},\omega) = 0 \tag{B7}$$

and

$$\sum_{\beta,\gamma=r,\varphi,z} \epsilon_{\alpha\beta\gamma}\nabla_\beta\, {}^{\parallel}G_{\gamma z}(\mathbf{r},\mathbf{R},\omega) = 0\,, \tag{B8}$$

where $\epsilon_{\alpha\beta\gamma}$ is the totally antisymmetric unit tensor of rank 3. Keeping Eqs. (B7) and (B8) in mind, Eq. (B6) is rewritten to give two independent equations for the transverse and longitudinal Green tensors of the form

$$\left(\Delta + k^2\right){}^{\perp}G_{zz}(\mathbf{r},\mathbf{R},\omega) = -\delta^{\perp}_{zz}(\mathbf{r}-\mathbf{R})\,, \tag{B9}$$

$$k^2\, {}^{\parallel}G_{zz}(\mathbf{r},\mathbf{R},\omega) = -\delta^{\parallel}_{zz}(\mathbf{r}-\mathbf{R}) \tag{B10}$$

with the delta-functions given by Eqs. (12) and (13) and ${}^{\perp(\parallel)}G_{zz}$ defined by Eq. (32).

The transverse Green function ${}^{\perp}G_{zz}(\mathbf{r},\mathbf{r}_A,\omega)$ was derived and analyzed in our previous work [10]. Its differential form equivalent to Eq. (32) is given by

$${}^{\perp}G_{zz}(\mathbf{r},\mathbf{r}_A,\omega) = \left(\frac{1}{k^2}\nabla_z\nabla_z + 1\right) g(\mathbf{r},\mathbf{r}_A,\omega) \tag{B11}$$

with $g(\mathbf{r},\mathbf{r}_A,\omega)$ being the Green function of the scalar Helmholtz equation, satisfying the radiation condition at infinity and boundary conditions on the CN surface. Indeed, substituting Eq. (B11) into Eq. (B9) and using Eq. (B7), one straightforwardly obtains

$$\left(\Delta + k^2\right) g(\mathbf{r},\mathbf{r}_A,\omega) = -\delta^{\perp}_{zz}(\mathbf{r}-\mathbf{r}_A)\,, \tag{B12}$$

the scalar Helmholtz equation with a transverse δ-source. For the longitudinal Green function ${}^{\parallel}G_{zz}(\mathbf{r},\mathbf{r}_A,\omega)$, one analogously has

$${}^{\parallel}G_{zz}(\mathbf{r},\mathbf{r}_A,\omega) = -\frac{1}{k^2}\nabla_z\nabla_z\, g(\mathbf{r},\mathbf{r}_A,\omega)\,, \tag{B13}$$

which upon substituting into Eq. (B10) yields

$$\nabla_z\nabla_z\, g(\mathbf{r},\mathbf{r}_A,\omega) = \delta^{\parallel}_{zz}(\mathbf{r}-\mathbf{r}_A)\,. \tag{B14}$$

The complete solution of Eq. (B11), which satisfies the radiation condition at infinity and boundary conditions on the CN surface, has for $r_A \geq r > R_{cn}$ the form [10]

$$g(\mathbf{r},\mathbf{r}_A,\omega) = g_0(\mathbf{r},\mathbf{r}_A,\omega) - \frac{R_{cn}}{(2\pi)^2}\sum_{p=-\infty}^{\infty} e^{ip\varphi}\int_C \frac{\beta(\omega)\, v^2 I_p^2(vR_{cn})K_p(vr_A)K_p(vr)}{1+\beta(\omega)\, v^2 R_{cn} I_p(vR_{cn})K_p(vR_{cn})}\, e^{ihz}dh\,, \tag{B15}$$

where the coordinate system has been fixed as is shown in Fig. 1, so that $\mathbf{r}_A = \{r_A, 0, 0\}$ and $\mathbf{r} = \{r, \varphi, z\}$, the first item is the particular solution of the inhomogeneous equation which is

$$g_0(\mathbf{r},\mathbf{r}_A,\omega) = \frac{1}{4\pi}\frac{e^{ik|\mathbf{r}-\mathbf{r}_A|}}{|\mathbf{r}-\mathbf{r}_A|}\,, \tag{B16}$$

the point-source function (see, e.g., Ref. [14]), and the second item is the general solution of the homogeneous equation with the boundary conditions imposed on the CN surface and at infinity. This latter item is represented in terms of the modified cylindric Bessel functions I_p and K_p with $v = v(h,\omega) = \sqrt{h^2-k^2}$ and $\beta(\omega) = 4\pi i\sigma_{zz}(R_{cn},\omega)/\omega$. The integration contour C goes along the real axis of the complex plane and envelopes the branch points $\pm k$ of the integrand from below and from above, respectively. The function $g(\mathbf{r},\mathbf{r}_A,\omega)$ for $r \leq r_A < R_{cn}$ is obtained from Eq. (B15) by means of a simple symbol replacement $I_p \leftrightarrow K_p$ in the numerator of the integrand.

Now, using Eqs. (B11), (B13), (B7) and the property $g(\mathbf{r},\mathbf{r}_A,\omega) = g(\mathbf{r}_A,\mathbf{r},\omega)$ which is obvious from Eqs. (B15) and (B16), it is not difficult to prove that

$${}^{\perp}G^{\perp}_{zz}(\mathbf{r}_A,\mathbf{r}_A,\omega) \;=\; {}^{\perp}G_{zz}(\mathbf{r}_A,\mathbf{r}_A,\omega)\,, \tag{B17}$$

$${}^{\parallel}G^{\parallel}_{zz}(\mathbf{r}_A,\mathbf{r}_A,\omega) \;=\; {}^{\parallel}G_{zz}(\mathbf{r}_A,\mathbf{r}_A,\omega)\,, \tag{B18}$$

$${}^{\perp}G^{\parallel}_{zz}(\mathbf{r}_A,\mathbf{r}_A,\omega) \;=\; 0\,, \tag{B19}$$

whereupon, making use of the definitions (35), (36) and Eqs. (38)–(42), one arrives for $r_A > R_{cn}$ at the the transverse and longitudinal local photonic DOS functions of the form

$$\overline{\xi}^{\perp}(\mathbf{r}_A,\omega) = \frac{3R_{cn}}{2\pi k^3}\,\mathrm{Im}\sum_{p=-\infty}^{\infty}\int_C \frac{dh\,\beta(\omega)\, v^4 I_p^2(vR_{cn})K_p^2(vr_A)}{1+\beta(\omega)\, v^2 R_{cn} I_p(vR_{cn})K_p(vR_{cn})}\,, \tag{B20}$$

$$\overline{\xi}^{\parallel}(\mathbf{r}_A,\omega) = \frac{3R_{cn}}{2\pi k^3}\,\mathrm{Im}\sum_{p=-\infty}^{\infty}\int_C \frac{dh\,\beta(\omega)\, h^2 v^2 I_p^2(vR_{cn})K_p^2(vr_A)}{1+\beta(\omega)\, v^2 R_{cn} I_p(vR_{cn})K_p(vR_{cn})}\,. \tag{B21}$$

Here, the sign in front of Eq. (B21) has been changed to be positive. This reflects the fact that the right-hand sides of Eqs. (B12) and (B14) are of opposite signs. As a consequence, partial solutions of the corresponding homogeneous equations should be taken to have opposite signs as well. This yields a correct (positive) sign of the longitudinal local photonic DOS which, along with the transverse local photonic DOS, must be a positively defined function. For $r_A < R_{cn}$, Eqs. (B20) and (B21) should be modified by the replacement $r_A \leftrightarrow R_{cn}$ in the Bessel function arguments in the numerators of the integrands. In dimensionless variables (47), these equations are rewritten to give Eqs. (49) and (50).

Finally, based upon the properties (B17)–(B19), one can easily prove Eqs. (33) and (34) for the dipole interaction matrix elements. The proof of Eq. (33) is straightforward. In view of Eq. (31), one has

$$\int d\mathbf{R}\,|\mathrm{g}^{\perp(\parallel)}(\mathbf{r}_A,\mathbf{R},\omega)|^2 = \pi\hbar\omega\frac{16\omega_A^2 d_z^2}{c^4}\int d\mathbf{R}\,\mathrm{Re}\,\sigma_{zz}(\mathbf{R},\omega) \times {}^{\perp(\parallel)}G_{zz}(\mathbf{r}_A,\mathbf{R},\omega)\,{}^{\perp(\parallel)}G_{zz}(\mathbf{r}_A,\mathbf{R},\omega)^*. \quad \text{(B22)}$$

Using further the integral relationship

$$\mathrm{Im}\,G_{\alpha\beta}(\mathbf{r},\mathbf{r}',\omega) = \frac{4\pi}{c}\,k \times\int d\mathbf{R}\,\mathrm{Re}\,\sigma_{zz}(\mathbf{R},\omega)G_{\alpha z}(\mathbf{r},\mathbf{R},\omega)G_{\beta z}(\mathbf{r}',\mathbf{R},\omega)^* \quad \text{(B23)}$$

[which is nothing but a particular 2D case of a general integral relationship proven for any 3D electromagnetic field Green tensor in Ref. [16], with Eq. (4) taken into account], one obtains for the right-hand side of Eq. (B22)

$$\hbar\frac{4\omega_A^2 d_z^2}{c^2}\,\mathrm{Im}^{\perp(\parallel)}G_{zz}^{\perp(\parallel)}(\mathbf{r}_A,\mathbf{r}_A,\omega),$$

whereupon using Eqs. (35), (36) and (38), one arrives at Eq. (33).

The proof of Eq. (34) is based upon Eq. (33). In view of this equation, the right-hand side of Eq. (34) takes the form

$$\int d\mathbf{R}\,|\mathrm{g}^{(\pm)}(\mathbf{r}_A,\mathbf{R},\omega)|^2 = \frac{(\hbar\omega_A)^2}{2\pi\omega^2}\,\Gamma_0(\omega) \times\left[\xi^{\perp}(\mathbf{r}_A,\omega)+\left(\frac{\omega}{\omega_A}\right)^2\xi^{\parallel}(\mathbf{r}_A,\omega)\right] \quad \text{(B24)}$$
$$\pm\frac{\omega}{\omega_A}\,2\mathrm{Re}\int d\mathbf{R}\,\mathrm{g}^{\perp}(\mathbf{r}_A,\mathbf{R},\omega)\,\mathrm{g}^{\parallel}(\mathbf{r}_A,\mathbf{R},\omega)^*,$$

where the last item can be further rewritten in terms of Eqs. (31), (32) and (B23) to give

$$\hbar\frac{8\omega\omega_A d_z^2}{c^2}\,\mathrm{Im}\,{}^{\perp}G_{zz}^{\parallel}(\mathbf{r}_A,\mathbf{r}_A,\omega)\,,$$

which is zero, according to Eq. (B19). Thus, one arrives at Eq. (34).

APPENDIX C: THE RELATION OF EQ.(48) WITH THE CASIMIR-POLDER FORMULA

In deriving an 'infinitely conducting plane' result (the Casimir-Polder formula [27]) from our theory, we will follow a general line of the work by Marvin and Tiogo [37] who did the same within the framework of their linear response theory.

We start with our weak-coupling-regime equation (54). First of all one has to simplify the local DOS functions $\overline{\xi}^{\perp(\parallel)}(\mathbf{r}_A,x)$ in this equation by putting $\overline{\sigma}_{zz}\to\infty$. From Eqs. (49) and (50), one has then for $r_A > R_{cn}$

$$\left\{\begin{array}{c}\overline{\xi}^{\perp}(\mathbf{r}_A,x)\\ \overline{\xi}^{\parallel}(\mathbf{r}_A,x)\end{array}\right\} = \frac{3}{\pi}\,\mathrm{Im}\int_0^\infty dy\left\{\begin{array}{c}y^2-1-i\varepsilon\\ y^2\end{array}\right\}\sum_{p=-\infty}^{\infty}\frac{K_p^2[\sqrt{y^2-1-i\varepsilon}\,u(r_A)x]I_p[\sqrt{y^2-1-i\varepsilon}\,u(R_{cn})x]}{K_p[x\sqrt{y^2-1-i\varepsilon}\,u(R_{cn})x]}\,, \quad \text{(C1)}$$

where ε is an infinitesimal positive constant which is necessary to correctly envelope the branch points of the integrand in integrating over y.

The next step is taking a large radius limit in Eq. (C1). This can be done by using the relationship

$$\lim_{\substack{a\to\infty\\ b\to\infty\\ (a-b=const)}}\sum_{n=-\infty}^{\infty}\frac{K_n^2(a)I_n(b)}{K_n(b)} = K_0[2(a-b)]$$

proved in Ref. [37]. One has

$$\left\{\begin{array}{c}\overline{\xi}^{\perp}(\mathbf{r}_A,x)\\ \overline{\xi}^{\parallel}(\mathbf{r}_A,x)\end{array}\right\} = \frac{3}{\pi}\,\mathrm{Im}\int_0^\infty dy\left\{\begin{array}{c}y^2-1-i\varepsilon\\ y^2\end{array}\right\} \times K_0[2\mu x\sqrt{y^2-1-i\varepsilon}\,]\,, \quad \text{(C2)}$$

where $\mu = 2\gamma_0 l/\hbar c$ with $l = r_A - R_{cn}$ being the atom-surface distance. The integration variable y in this equation contains implicit frequency dependence. Indeed,

comparing dimensionless equations (49), (50) with (B20), (B21), one can see that $y = h/k = h(c/\omega) = h(c\hbar/2\gamma_0 x)$. For the following it makes sense to extract this frequency dependence by the substitution $y = \tau/x$ with dimensionless $\tau = h(c\hbar/2\gamma_0)$. The result takes the form

$$\overline{\xi}^{\perp(\parallel)}(\mathbf{r}_A, x) = \frac{3}{2i\pi x}\left\{f^{\perp(\parallel)}(\mathbf{r}_A, x) - f^{\perp(\parallel)}(\mathbf{r}_A, x)^*\right\} \tag{C3}$$

with

$$\left\{\begin{array}{c} f^{\perp}(\mathbf{r}_A, x) \\ f^{\parallel}(\mathbf{r}_A, x) \end{array}\right\} = \int_0^\infty d\tau \left\{\begin{array}{c} (\tau/x)^2 - 1 - i\varepsilon \\ (\tau/x)^2 \end{array}\right\} \times K_0[2\mu x\sqrt{(\tau/x)^2 - 1 - i\varepsilon}\,]\,. \tag{C4}$$

Substituting Eq. (C3) into Eq. (54), one has

$$\varepsilon_{vw}(\mathbf{r}_A) = \frac{3x_A}{4i\pi^2} \times\left\{\int_0^\infty \frac{dx\,\tilde{\Gamma}_0(x)}{(x_A + x)x^2}\left[f^{\perp}(\mathbf{r}_A, x) - \frac{x}{x_A}f^{\parallel}(\mathbf{r}_A, x)\right] - \int_0^{-\infty}\frac{dx\,\tilde{\Gamma}_0(x)}{(x_A - x)x^2}\left[f^{\perp}(\mathbf{r}_A, -x)^* + \frac{x}{x_A}f^{\parallel}(\mathbf{r}_A, -x)^*\right]\right\}. \tag{C5}$$

Here, in the second item, the change of the integration variable from x to $-x$ has been made and it has been taken into account that $\tilde{\Gamma}_0(-x) = -\tilde{\Gamma}_0(x)$. Noting further that both integrands in Eq. (C5) do not have poles in the upper complex half plane, one may rotate the integration path of the first and the second integral by $\pi/2$ and by $-\pi/2$, respectively. Then, both integrals become the integrals over the positive imaginary axis of the complex plane and Eq. (C5) takes the form

$$\varepsilon_{vw}(\mathbf{r}_A) = \frac{3x_A}{4i\pi^2} \times\left\{\int_0^{i\infty} \frac{dz\,\tilde{\Gamma}_0(z)}{(x_A + z)z^2}\left[f^{\perp}(\mathbf{r}_A, z) - \frac{z}{x_A}f^{\parallel}(\mathbf{r}_A, z)\right] - \int_0^{i\infty}\frac{dz\,\tilde{\Gamma}_0(z)}{(x_A - z)z^2}\left[f^{\perp}(\mathbf{r}_A, -z)^* + \frac{z}{x_A}f^{\parallel}(\mathbf{r}_A, -z)^*\right]\right\}. \tag{C6}$$

Making further the change of the integration variable from z to iu with real non-negative u, one arrives at

$$\varepsilon_{vw}(\mathbf{r}_A) = \frac{3x_A}{4\pi^2} \times\left\{-\int_0^{\infty} \frac{du\,\tilde{\Gamma}_0(iu)}{(x_A + iu)u^2}\left[f^{\perp}(\mathbf{r}_A, iu) - \frac{iu}{x_A}f^{\parallel}(\mathbf{r}_A, iu)\right] + \int_0^{\infty}\frac{du\,\tilde{\Gamma}_0(iu)}{(x_A - iu)u^2}\left[f^{\perp}(\mathbf{r}_A, -iu)^* + \frac{iu}{x_A}f^{\parallel}(\mathbf{r}_A, -iu)^*\right]\right\}. \tag{C7}$$

Here, the functions $f^{\perp(\parallel)}(\mathbf{r}_A, iu)$ have the following explicit form

$$\left\{\begin{array}{c} f^{\perp}(\mathbf{r}_A, iu) \\ f^{\parallel}(\mathbf{r}_A, iu) \end{array}\right\} = -u\int_1^\infty d\eta \left\{\begin{array}{c} \eta^3/\sqrt{\eta^2 - 1} \\ \eta\sqrt{\eta^2 - 1} \end{array}\right\} K_0(2\mu u\eta) \tag{C8}$$

obtained from Eq. (C4) after the change of the integration variable by the subsequent substitutions $x = iu$ and $\eta^2 = \tau^2/u^2 + 1$. The functions $f^{\perp(\parallel)}(-iu)^* = f^{\perp(\parallel)}(iu)$ as a consequence of a general property $K_\nu(z)^* = K_\nu(z^*)$ [26]. Substituting Eq. (C8) into Eq. (C7) and making allowance for the fact that $\tilde{\Gamma}_0(iu) = -i\tilde{\Gamma}_0(u)$, one further has

$$\varepsilon_{vw}(\mathbf{r}_A) = -\frac{3x_A}{2\pi^2}\int_0^\infty \frac{du\,\tilde{\Gamma}_0(u)}{x_A^2 + u^2} \times\int_1^\infty d\eta\,\eta\left(\sqrt{\eta^2 - 1} + \frac{\eta^2}{\sqrt{\eta^2 - 1}}\right)K_0(2\mu u\eta)\,, \tag{C9}$$

which upon the substitution $\eta^2 = \rho$ becomes

$$\varepsilon_{vw}(\mathbf{r}_A) = -\frac{3x_A}{4\pi^2}\int_0^\infty \frac{du\,\tilde{\Gamma}_0(u)}{x_A^2 + u^2} \times\int_1^\infty d\rho\left(\sqrt{\rho - 1} + \frac{\rho}{\sqrt{\rho - 1}}\right)K_0(2\mu u\sqrt{\rho}\,)\,. \tag{C10}$$

In Eq. (C10), the first integral over ρ is taken exactly by means of the relationship [38]

$$\int_1^\infty d\rho\sqrt{\rho - 1}\,K_0(a\sqrt{\rho}\,) = \sqrt{\frac{2\pi}{a^3}}\,K_{3/2}(a) \underset{a\to\infty}{\longrightarrow} \frac{\pi}{a^3}(1 + a)e^{-a}$$

and the second one – by making a large argument series expansion of the integrand and its subsequent termwise integration. This, upon returning back to dimensional variables by means of Eqs. (47) and using the definition (see, e.g., [39])

$$\alpha_{zz}(iu) = \frac{2}{\hbar}\,\frac{d_z^2\,\omega_A}{\omega_A^2 - (iu)^2}$$

for the polarizability tensor zz-component of the two-level system, finally yields

$$E_{vw}(\mathbf{r}_A) \;\approx\; -\frac{\hbar}{8\pi l^3}\int_0^\infty du\,\alpha_{zz}(iu) \;\times\; \left[1 + 2\frac{u}{c}\,l + 2\left(\frac{u}{c}\right)^2 l^2\right] e^{-2(u/c)l}.$$

This is the half of the well-known Casimir-Polder result for the vdW energy of an atom near an infinitely conducting plane (see Refs. [27, 37]), in agreement with the fact that our model of the atom-electromagnetic-field interactions in the presence of a nanotube only takes the longitudinal (along the nanotube axis, or, equivalently, parallel to the plane in the large nanotube radius limit) atomic dipole orientation into account. Another half of the Casimir-Polder vdW energy would come from the transverse (perpendicular to the plane) atomic dipole orientation which we have neglected.

[1] M.S. Dresselhaus, G. Dresselhaus, and P.C. Eklund, *Science of Fullerens and Carbon Nanotubes* (Academic Press, New York, 1996).

[2] H. Dai, Surf. Sci. **500**, 218 (2002).

[3] R.H. Baughman, A.A. Zakhidov, and W.A. de Heer, Science **297**, 787 (2002).

[4] L. Duclaux, Carbon **40**, 1751 (2002).

[5] G.-H. Jeong, A.A. Farajian, R. Hatakeyama, T. Hirata, T. Yaguchi, K. Tohji, H. Mizuseki, and Y. Kawazoe, Phys. Rev. B **68**, 075410 (2003).

[6] H. Shimoda, B. Gao, X.P. Tang, A. Kleinhammes, L. Fleming, Y. Wu, and O. Zhou, Phys. Rev. Lett. **88**, 015502 (2002).

[7] M.M. Calbi, M.W. Cole, S.M. Gatica, M.J. Bojan, and G. Stan, Rev. Mod. Phys. **73**, 857 (2001).

[8] I.V. Bondarev, G.Ya. Slepyan, and S.A. Maksimenko, Phys. Rev. Lett. **89**, 115504 (2002).

[9] I.V. Bondarev and Ph. Lambin, Phys. Lett. A **328**, 235 (2004).

[10] I.V. Bondarev and Ph. Lambin, Phys. Rev. B **70**, 035407 (2004).

[11] S.Y. Buhmann, H.T. Dung, and D.-G. Welsch, J. Opt. B: Quantum Semiclass. Opt. **6**, S127 (2004).

[12] S.Y. Buhmann, H.T. Dung, L. Knöll, and D.-G. Welsch, quant-ph/0403128.

[13] L.A. Girifalco and M. Hodak, Phys. Rev. B **65**, 125404 (2002).

[14] A.S. Davydov, *Quantum Mechanics* (Pergamon, New York, 1976).

[15] H.T. Dung, L. Knöll, and D.-G. Welsch, Phys. Rev. A **62**, 053804 (2000).

[16] L. Knöll, S. Scheel, and D.-G. Welsch, in: *Coherence and Statistics of Photons and Atoms*, edited by J. Peřina (Wiley, New York, 2001).

[17] G.Ya. Slepyan, S.A. Maksimenko, A. Lakhtakia, O. Yevtushenko, and A.V. Gusakov, Phys. Rev. B 60, 17136 (1999).

[18] S. Tasaki, K. Maekawa, and T. Yamabe, Phys. Rev. B **57**, 9301 (1998).

[19] Z.M. Li, Z.K. Tang, H.J. Liu, N. Wang, C.T. Chan, R. Saito, S. Okada, G.D. Li, J.S. Chen, N. Nagasawa, and S. Tsuda, Phys. Rev. Lett. **87**, 127401 (2001).

[20] A. Jorio, A.G. Souza Filho, V.W. Brar, A.K. Swan, M.S. Ünlü, B.B. Goldberg, A. Righi, J.H. Hafner, C.M. Lieber, R. Saito, G. Dresselhaus, and M.S. Dresselhaus, Phys. Rev. B **65**, 121402R (2002).

[21] A.G. Marinopoulos, L. Reining, A. Rubio, and N. Vast, Phys. Rev. Lett. **91**, 046402 (2003).

[22] W. Vogel, D.-G. Welsch and S. Wallentowitz, *Quantum Optics: an Introduction* (Wiley-VCH, New York, 2001).

[23] A.A. Abrikosov, L.P. Gorkov, and I.E. Dzyaloshinski, *Methods of Quantum Field Theory in Statistical Physics* (Dover, New York, 1975).

[24] L. Allen and J. H. Eberly, *Optical Resonance and Two-Level Atoms* (Wiley, New York, 1975).

[25] M. Florescu and S. John, Phys. Rev. A **64**, 033801 (2001).

[26] *Handbook of Mathematical Functions*, eds. M. Abramovitz and I.A. Stegun (Dover, New York, 1972).

[27] H.B.G. Casimir and D. Polder, Phys. Rev. **73**, 360 (1948).

[28] H. Schniepp and V. Sandoghdar, Phys. Rev. Lett. **89**, 257403 (2002).

[29] D.R. Lide (Editor-in-Chief), *Handbook of Chemistry and Physics* (CRC Press, New York, 1999).

[30] K. Masenelli-Varlot, E. McRae, and N. Dupont-Pavlovsky, Appl. Surf. Sci. **196**, 209 (2002).

[31] C. Weisbuch, M. Nishioka, A. Ishikawa, and Y. Arakawa, Phys. Rev. Lett. **69**, 3314 (1992).

[32] L.C. Andreani, G. Panzarini, and J.-M. Gerard, Phys. Rev. B **60**, 13276 (1999).

[33] D. Dini, R. Köhler, A. Tredicucci, G. Biasiol, and L. Sorba, Phys. Rev. Lett. **90**, 116401 (2003).

[34] S. Haroche and D. Kleppner, Phys. Today **42**, No. 1, 24 (1989).

[35] J.M. Raimond, M. Brune, and S. Haroche, Rev. Mod. Phys. **73**, 565 (2001).

[36] J.D. Jackson, *Classical Electrodynamics* (Wiley, New York, 1975).

[37] A.M. Marvin and F. Toigo, Phys. Rev. A **25**, 782 (1982).

[38] I.S. Gradshteyn and I.M. Ryzhik, *Tables of Integrals, Series and Products* (Academic, New York, 1965).

[39] G.S. Agarwal, Phys. Rev. A **11**, 243 (1975).

[40] One should make a clear difference between this definition and that where the strong (weak) atom-field coupling regime is defined as that violating (non-violating) the applicability domain of the Markovian approximation [25]. Our definition here is based on the Born approximation associated with the strength of the coupling between the atom and the photonic reservoir, whereas the Markovian approximation is related to memory effects of the photonic reservoir.